

Characterization of Temperature Dependent Mechanical Behavior of Cartilage

YongSeok Chae, MS,^{1,2} Guillermo Aguilar, PhD,^{2,3} Enrique J. Lavernia, PhD,^{1,3,4} and Brian J.F. Wong, MD, PhD^{2,3,5*}

¹Department of Chemical Engineering and Materials Science, The Henry Samueli School of Engineering, University of California, Irvine, California 92697-2575

²The Beckman Laser Institute and Medical Clinic, University of California, Irvine, 1002 Health Sciences Road East, Irvine, California 92612

³Department of Biomedical Engineering, The Henry Samueli School of Engineering, University of California, Irvine, California 92697-2575

⁴Department of Chemical Engineering and Materials Science, College of Engineering, University of California, Davis, California 95616

⁵Department of Otolaryngology-Head and Neck Surgery, University of California, Irvine, 101 The City Drive, Orange, California 92668

Background and Objectives: Few quantitative studies have investigated the temperature dependent viscoelastic properties of cartilage tissue. Cartilage softens and can be reshaped when heated using laser, RF, or contact heating sources. The objectives of this study were to: (1) measure temperature dependent flexural storage moduli and mechanical relaxation in cartilage, (2) determine the impact of tissue water content and orientation on these mechanical properties, and (3) use these measurements to estimate the activation energy associated with the mechanical relaxation process.

Study Design/Materials and Methods: Porcine nasal septal cartilage specimens (30 × 10 × 2 mm) were deformed using a single cantilever arrangement in a dynamic thermomechanical analyzer. Stress relaxation measurements were made at discrete temperatures ranging from 25 to 70°C in response to cyclic deformation (within the linear viscoelastic region). The time and temperature dependent behavior of cartilage was measured using frequency multiplexing techniques (10–64 Hz), and these results were used to estimate the activation energy for the phase change using the Williams–Landel–Ferry (WLF) equation and the Arrhenius kinetic equation. In addition, the effect of tissue orientation was examined with specimens oriented in both transverse and longitudinal directions at room temperature.

Results: The storage moduli of porcine cartilage decreased with increasing temperature, and a critical change in mechanical properties was observed between 58 and 60°C with a reduction in the storage modulus by 85–90%. The shift of the stress relaxation behavior from viscoelastic solid to viscoelastic liquid was observed between 50 and 57°C and likely corresponds to the transition temperature region in which structural changes in the tissue occur. The storage moduli for transverse and longitudinally oriented specimens were 19–22 and 14–16 MPa, respectively at ambient temperature. Reducing the water content (<10% mass loss) by allowing it to dry under ambient conditions resulted

in reduction in the storage modulus by 31–36%. The activation energy associated with the mechanical relaxation of cartilage was 147 kJ/mole at 60°C. This value was calculated by measuring stress–strain relationship under conditions where linear viscoelastic behavior was observed (0.09–0.15% of strain) within the transition temperature region (58–60°C).

Conclusions: The anisotropic mechanical behavior of cartilage was quantitatively analyzed in the transversely and longitudinally oriented specimens. Viscoelastic behavior appeared to be strongly dependent on the water content. Using empirically determined estimates of the transition zone temperature range accompanying stress relaxation, the activation energy for stress relaxation was calculated using time and temperature superposition theory and WLF equation. Further investigation of the molecular changes, which occur during laser irradiation, may assist in understanding the thermal and mechanical behavior of cartilage and how the reshaping process might be optimized. *Lasers Surg. Med.* 32:271–278, 2003.

© 2003 Wiley-Liss, Inc.

Key words: stress relaxation; cartilage reshaping; dynamic mechanical analyzer; flexural storage modulus; WLF equation; Arrhenius relation; activation energy; shift factor; biomechanics; plastic surgery; otolaryngology

Contract grant sponsor: The US Air Force Office of Scientific Research; Contract grant sponsor: The National Institutes of Health; Contract grant numbers: DC 00170, HD-42057; Contract grant sponsor: The Office of Naval Research; Contract grant number: N00014-94-0874; Contract grant sponsor: The Air Force Office of Scientific Research; Contract grant sponsor: National Science Foundation; Contract grant number: NSF DMR-0076498.

*Correspondence to: Dr. Brian J.F. Wong, MD, PhD, The Beckman Laser Institute, University of California-Irvine, 1002 Health Sciences Road East, Irvine, CA 92612.

E-mail: bjfwong@io.bli.uci.edu

Accepted 3 February 2003

Published online in Wiley InterScience

(www.interscience.wiley.com).

DOI 10.1002/lsm.10167

INTRODUCTION

Free autologous cartilage grafts are used extensively in plastic surgery of the head and neck with donor specimens harvested from the pinna of the ear, nasal septum, or rib. In as much as the shape of donor cartilage grafts may not meet the geometrical demands required at the recipient site, reshaping of cartilage by carving, suturing, or morselizing is often necessary. Unfortunately, these traditional techniques can result in damage to the transplanted tissue and decrease viability. Furthermore, the physical manipulation of the tissue may alter graft resilience and weaken the tissue.

Laser assisted reshaping of cartilage is a new surgical procedure designed to allow in-situ treatment of deformities with less morbidity than traditional procedures [1–13]. During laser irradiation, mechanically deformed cartilage undergoes a subtle change in material properties that permits tissue to be reshaped into new stable configurations [5,6,11,12,14–22]. Although the mechanism responsible for shape change has not been conclusively established, the process is thought to involve a combination of collagen denaturation, alteration of weak van der Waals bonds between proteoglycan molecules, and/or water flux [9,18].

Sobol et al. has suggested an intriguing hypothesis that the underlying mechanism behind laser reshaping is a consequence of a phase transformation of bound water to free water in the cartilage matrix, which takes place at a temperature of approximately 70°C [18]. The alteration in internal stress during laser irradiation results in accelerated stress relaxation and represents a fundamental biophysical change that results in cartilage reshaping [18,23,24]. Preliminary studies using diffuse light scattering and calorimetric measurements have identified changes in cartilage tissue, thermal and optical properties that are consistent with this phase transformation hypothesis [11–13,15,19,20,25–32].

Cartilage is a complex tissue composed of a three-dimensional collagen fibrillar framework containing a matrix of proteoglycan molecules that possess negatively charged ion groups (SO_3^- and COO^- moieties). Cartilage can be thought of as a charged hydrogel where all of the free space is filled with water, in either partially bound or free states. Polarized water molecules bind weakly to the negatively charged groups attached to both proteoglycan and collagen molecules. Free water likewise contains dissolved mineral substances including positively charged Na^+ and Ca^{2+} ions, which are attracted to negatively charged components of proteoglycan molecules; these ions are thus trapped in the matrix when free water is forced out of it during deformation or evaporation. The heterogeneous distribution of negatively charged groups in the polymeric proteoglycan chains account for the intra-molecular internal stresses of the tissue. It has been suggested that the stress relaxation of cartilages is a function of the average distance of mass transfer of proteoglycan subunits since the process may involve the successive adsorption and desorption of water by these structures [9]. Water may play

a significant role in the reshaping process since evaporation occurs during laser irradiation (with a subsequent increase in the concentrations of collagen and other proteins within the matrix). It is well known that the degree of hydration greatly influences tissue ablation and shrinkage behavior [18,33,34]. Thus this hypothetical bound to free transition of water may increase the mobility of constitutive elements of the matrix, which may lead to stress relaxation.

In situ, the negatively charged proteoglycans are compressed and their expansion is resisted by tensile strength of the surrounding collagen framework. The multi-branched chained polymeric molecular structure of cartilage results in viscoelasticity, and underscores the importance of studying the time and temperature dependent behavior of this material during deformation.

In previous investigations, stress and strain during laser irradiation were measured in cartilage under tension [35] and cantilevered deformation [23,36] during Nd:YAG laser ($\lambda = 1.32 \mu\text{m}$) irradiation, under quasi-static conditions. More precise and detailed measurements of cartilage viscoelastic behavior are needed to further elucidate the mechanisms behind reshaping. In the rheological sciences, dynamic mechanical analysis (DMA) is widely used for characterizing viscoelastic materials (e.g., storage and loss modulus, damping properties) in response to sinusoidal deformations or loads.

Chae et al. [37] have previously determined that the thermal properties of cartilage change with tissue water content, and it is likely that the mechanical properties depend upon the water content of the tissue as well. Hence, examining the effect of water content on cartilage thermo-viscoelastic behavior is an important goal of this study. Characterizing time and temperature dependent changes in the elastic modulus of cartilage may have value in optimizing the process of laser reshaping even though laser heat generation in tissue occurs at a much faster rate. The objectives of this study are to: (1) measure temperature dependent flexural storage moduli and mechanical relaxation in cartilage and determine whether these properties depend upon specimen orientation, (2) examine the impact of tissue water content on these mechanical properties, and (3) use these measurements to estimate the activation energy associated with the mechanical relaxation process.

MATERIALS AND METHODS

Tissue Preparation

Crania from freshly sacrificed domestic pigs were obtained from a local packing house (Farmers John, Vernon, CA) and the nasal septal cartilages were harvested as described previously [38]. Cartilage grafts were cut into rectangular slabs measuring $30 \times 10 \text{ mm}$ with thickness of 1–2 mm. A commercial rotary food slicer (Model 620, Chef's Choice Intl., EdgeCraft Corp., Avondale, PA) was used to cut specimens to a uniform thickness and remove perichondrial tissue [35]. Specimens were oriented either longitudinally or transversely with respect to the long-axis of the septal cartilage (Fig. 1). The specimens were immersed

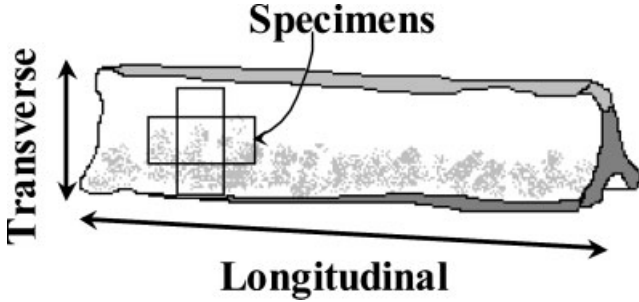


Fig. 1. Specimen of porcine septal cartilage with geometry and orientations.

in saline solution following harvest and processing. Mass was determined just before and after each experiment using a microbalance after excess surface water was removed by gently blotting with tissue paper.

Dynamic Mechanical Analysis (DMA)

Time dependent tissue mechanical properties were measured using a dynamic mechanical analyzer (DMA 2980, TA Instrument, Delaware, CA). The DMA relies upon measuring stress in a material in response to small oscillatory strains with the specimen secured in a variety of mechanical configurations. A single cantilever set-up was used for these studies, and measurements were performed under isothermal conditions varying from ambient to 80°C. DMA oscillation frequencies varied from 1 to 60 Hz. Deformation of a single beam cantilevered specimen produces a combination of both flexural and shear forces. In short thick specimen shear forces are dominant. In contrast, in long thin specimens, flexural deformation is the predominant mode, and the one of interest for the present studies. For instance, for a cartilage specimen with a length to thickness ratio of 10, shear stress contributes less than 5% and the deformation mode is virtually pure flexure. The rectangular cartilage specimens used here for the DMA experiments had a length to thickness ratio greater than 10.

The evaporation rate of water from cartilage was measured by placing specimens in the pan of a microbalance and allowing dehydration to occur under ambient conditions as a function of time. In addition, specimen mass was recorded before and after each experiment. The range of linear viscoelastic behavior was determined at ambient temperatures using a 1 Hz oscillation frequency on the DMA instrument. Each specimen was rapidly secured to the DMA head and sealed in the furnace, which was preheated to a user-defined set point temperature. This was done in order to rapidly establish thermal equilibrium between the specimen and furnace at the user-defined set point temperature. Inserting the specimen into the chamber at ambient temperatures and then heating to the set point would result in significant specimen dehydration and subject the tissue to a relatively slow ramp-heating curve. Ideally, the specimen, furnace, and DMA apparatus should reach set point temperature instantaneously, however,

methods that could accomplish this (high power infrared laser (IR), IR ovens, and microwave heating) are beyond the scope of this study.

Estimation of Time-Based Shift Factor and Activation Energy

The time-based shift factor [39] was measured using multi frequency sweep analysis (MFSA). In MFSA, a step and hold temperature profile is applied and a frequency sweep is made at each isothermal temperature. The degree of horizontal shifting (i.e., time) required to superimpose a given set of flexural moduli at one temperature onto a standard curve established at a set reference temperature (near the phase transition temperature) has been mathematically described, and the theory is described below.

Theory of Time-Temperature Superposition

In theoretical models of dilute solutions composed of flexible molecules based on the “bead-spring model” [39], the contribution of the solute to the storage and relaxation modulus is proportional to cRT/M , where c is the concentration and M is the molecular weight of the solute. Likewise, the relaxation time τ is proportional to $[\eta]\eta_s M/RT$, where $[\eta] = \lim_{C \rightarrow 0} (\eta_0 - \eta_s)/\eta_s C$ is the intrinsic viscosity, η_s is a viscosity of solvent, and η_0 is a steady state solution viscosity for the corresponding quantities extrapolated to infinite dilution. All the relaxation times formulated in terms of the intrinsic viscosity can be assumed to have the same temperature dependence based on an extrapolation to infinite dilution to eliminate quantities not directly measurable. Hence; the time based shift factor a_T (a function of temperature) can be conveniently represented by the ratio of any specific relaxation time τ_p at temperature T to its value at an arbitrary reference temperature T_0 :

$$\frac{(\tau_p)_T}{(\tau_p)_{T_0}} = a_T = \frac{([\eta]\eta_s)_T T_0}{([\eta]\eta_s)_{T_0} T} \quad (1)$$

The time base shift factor, a_T underscores the basic relationship between temperature and viscoelasticity.

A phase transition results from an increase of molecular mobility with rising temperature. This corresponds to the “expansion” of free volume, which may be present as holes on the order of molecular (monomeric) dimensions or smaller voids associated with packing irregularities. Free volume is defined as smaller voids associated with packing irregularities. Molecular mobility at any temperature depends primarily on the free volume remaining, so the rates of both bulk and shear deformations can be advantageously expressed in terms of free volume (v_f) rather than T as the independent variable.

$$\ln \eta_0 = \ln A + B(v - v_f)/v_f \quad (2)$$

In Equation 2, A and B are empirically determined constants [39]. Equation 2 can then be expressed in terms of the shift factor a_T , with the definition $f = v_f/v$ and $f \cong f_0 + \alpha_f(T - T_0)$, where f_0 is the fractional free volume

at an arbitrary reference temperature T_0 with $f_0 = B/2.303C_1$ and $\alpha_f = B/2.303C_1C_2$ [39].

$$\log(a_T) = \frac{B}{2.303} \left(\frac{1}{f} - \frac{1}{f_0} \right) = - \frac{(B/2.303f_0)(T - T_0)}{(f_0/\alpha_f) + (T - T_0)} \quad (3)$$

The amount of shifting along the horizontal (x) axis in a typical time–temperature superposition (TTS) is generally described using both the Williams–Landel–Ferry (WLF) equation

$$\log(a_T) = \frac{-C_1(T - T_0)}{C_2 + (T - T_0)} \quad (4)$$

and Arrhenius equation:

$$\ln a_T = \frac{E}{R(T - T_0)} \quad (5)$$

This TTS plot is required to align the individual experimental data points with points on the master curve (reference curve). In Equation 4, C_1 and C_2 are empirically determined constants ($C_1 = B/2.303f_0$, $C_2 = f_0/\alpha_f$), and T_0 is the reference temperature (in K). In Equation 5, E is the activation energy associated with the relaxation, R is the gas constant, and T is the measurement temperature (in K). We used a commercial software package (TTS Rheo advantage data analysis, TA Inst.) to calculate calibration constants (C_1 and C_2) and thus estimate the activation energy for stress relaxation in cartilage. The estimation of C_1 and C_2 depends on the dynamic storage moduli from each isothermal condition. The measurement of elastic moduli is dependent on the geometry of the specimen and the intrinsic limitations of each instrument.

RESULTS

Flexural Stress–Strain

Figure 2 shows representative stress/strain behavior in three cartilage slabs (1–3 mm thickness) during sinusoidal displacement (0.4% amplitude strain at 1 Hz) at three separate isothermal conditions (27, 55, and 65°C) in longitudinal orientation. To accurately determine mechanical properties, deformation must occur using displacement amplitudes that are within the linear viscoelastic region (e.g., material response is independent of the magnitude of the deformation). This linear region was determined using strain-sweep analysis. The linear viscoelastic behavior was observed with strains less than 0.145% at 27°C, 0.11% at 55°C, and 0.100% at 65°C. This latter measurement is at a higher temperature than the transition temperature (around 60°C) previously reported [37,40]. It should be noted that each curve in Figure 2 represents measurements obtained using a different specimen for each temperature. Regression lines (dotted) were calculated using the initial set of data points to provide an estimate of when stress and strain deviated from linear behavior. This was used to provide an estimate of the region of linear behavior.

Specimen Orientation and Effect of Water Content

The flexural storage moduli were measured within the linear elastic region (0.1% of strain) in both longitudinally

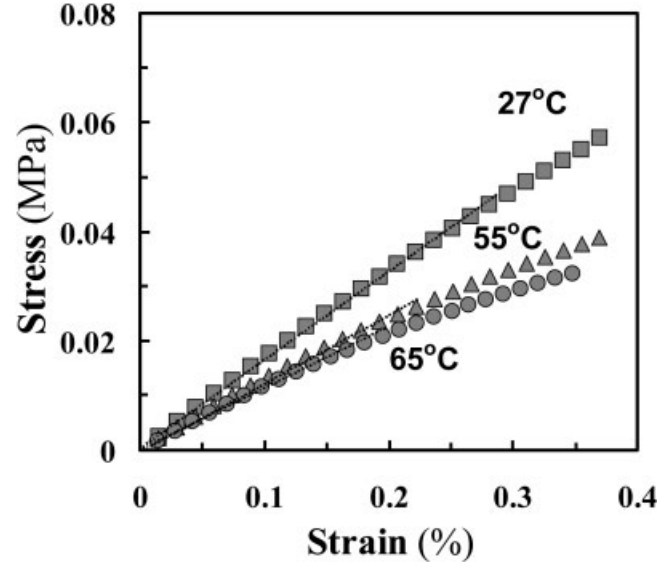


Fig. 2. Stress strain curve of porcine septal cartilage for linear viscoelastic behavior at isothermal temperature (27, 55, and 65°C).

and transversely oriented specimens at a constant temperature of 25°C at 1 Hz (Fig. 3). Since evaporation occurs during these experiments, specimen mass was recorded at selected time intervals during the experiments to gauge the impact of water loss. In Figure 3, curve (1) represents percent reduction in specimen mass (due to evaporation) as a function of time while curves (2) and (3) correspond to the storage modulus of transversely and longitudinally oriented specimens, respectively. Initial storage modulus of the transversely oriented cartilage specimen was 12.5–14.0 MPa and the longitudinal specimen was 18.0–19.5 MPa. The storage modulus was higher in

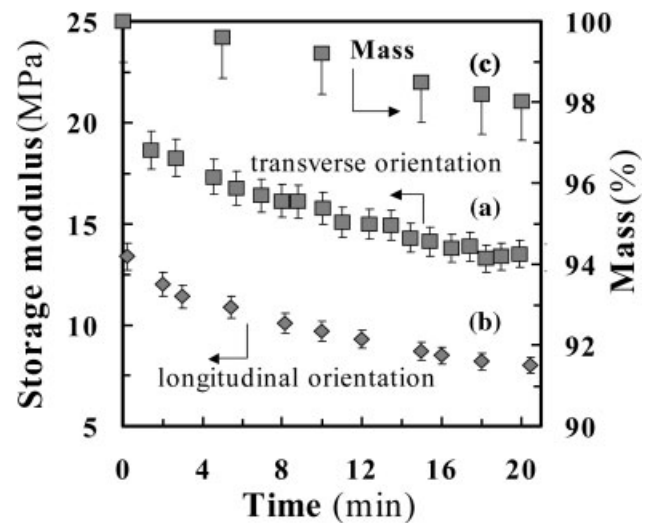


Fig. 3. Flexural storage modulus of porcine nasal septal cartilage; (a) transversal, (b) longitudinal, (c) orientation with mass loss.

transversely oriented specimens than in longitudinally oriented ones, and in both cases the modulus decreased with time as dehydration occurred. The difference in storage modulus between the two orientations was 30–38%. Similar reductions in elastic modulus in both transverse and longitudinal orientations at ambient temperature were observed. The constant of proportionality between storage moduli of longitudinal and transversely oriented specimens was estimated to be approximately 0.65–0.7. Mechanical anisotropy in cartilage can be characterized knowing these differences. Hence, measurements of material behavior in the transverse direction can be used to estimate material behavior in the longitudinal direction, and vice versa.

While these experiments are performed immediately after the specimen is removed from immersion in saline, water loss due to dehydration was a concern, which provided the motivation of measuring the impact of water content on tissue properties. After 5 minutes, the specimen mass was reduced only by about 1%, while the storage moduli decreased by 12 and 19% for transverse and longitudinally orientated specimens, respectively. Similarly, after 20 minutes, when mass loss reached 3%, the storage moduli decreased by 31 and 36% for transversely and longitudinally orientated specimens, respectively. These observations underscore the impact of even small reductions in water content on tissue mechanical properties.

Stress Relaxation of Porcine Nasal Cartilage

In Figure 4, multi frequency sweep analyses were used to obtain the flexural storage moduli at various frequencies (14, 23, 37, and 61 Hz) at different temperatures. The transition as evidenced by a reduction in instantaneous storage modulus of cartilage as temperature increased, and was more pronounced as temperature approached 60°C.

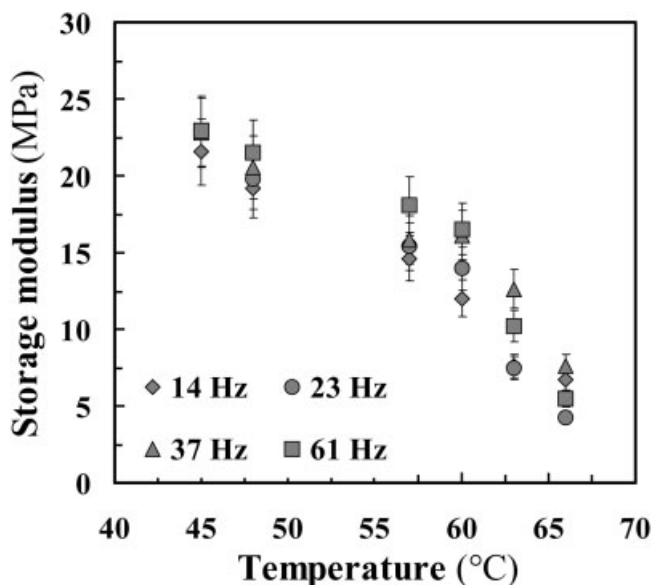


Fig. 4. Storage modulus of porcine septal cartilage versus temperature at various frequencies.

Figure 5 shows that the instantaneous storage modulus changes at approximately 55°C at 14 Hz. This relaxation event in cartilage started at about 50°C with the storage modulus gradually falling until a value of 2–3 MPa is reached at 65°C. These results are consistent with those illustrated in Figure 4.

The error bars in Figure 4 represent the standard error derived from a limited number of samples, 3 or 4. This suggests that the temperature transition region associated with the relaxation of cartilage is between 50 and 65°C, which is similar to the temperature range where changes in heat capacity of cartilage were identified using differential scanning calorimetry [40]. In the transition temperature region, the instantaneous storage modulus rapidly dropped by 80–85%. Above 70°C, the magnitude of the change in the storage modulus was observed to be within the instrument error range (0.3–0.5 MPa), which is largely due to specimen clamp related effects. Reproducible and accurate measurements above 70°C were not obtained because the evaporation rate increased rapidly.

Figure 6 shows normalized relaxation storage moduli versus time for specific temperatures. Above 50°C, the relaxation modulus decreases rapidly within 1 minute and then slowly approached an equilibrium value. At temperatures below 50°C, elastic energy is still stored in the tissue matrix, which is under constant flexural strain. This energy very slowly dissipates, and asymptotically approaches a final non-zero value. In contrast, at 57°C and above, the dissipation of stored elastic energy is rapid and complete mechanical relaxation of the tissue is observed (e.g., the normalized relaxation modulus reaches zero). These results demonstrate that cartilage can continue to store elastic energy below 50°C, but above this temperature threshold, complete mechanical relaxation occurs over a much shorter time interval with dissipation of any stored

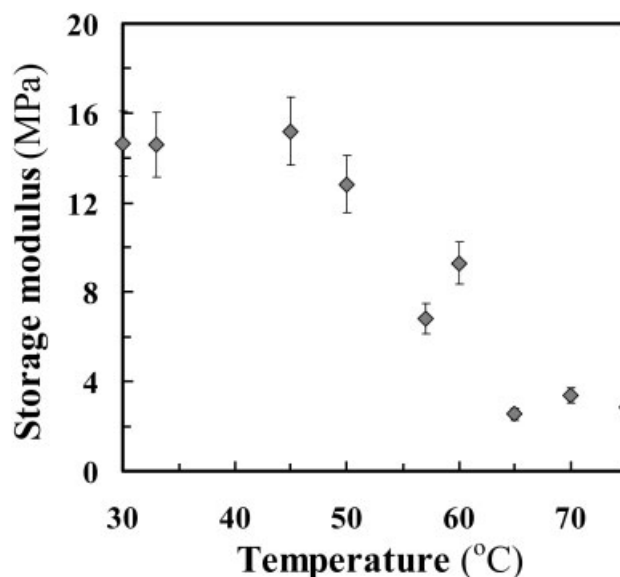


Fig. 5. Storage modulus of porcine nasal septal cartilage at various temperatures in longitudinal orientation.

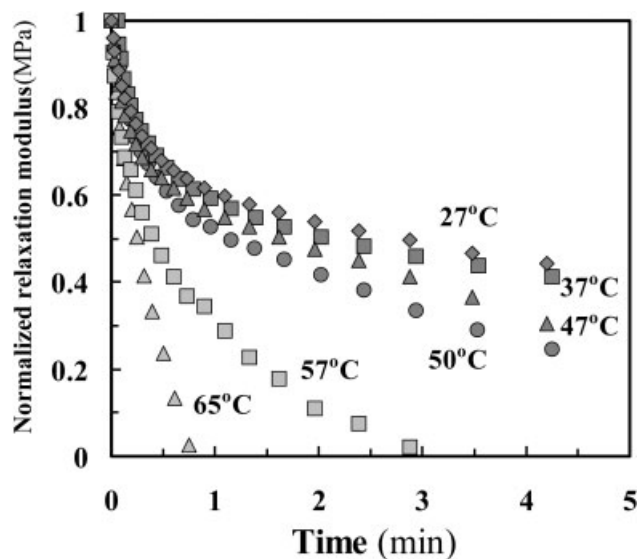


Fig. 6. Stress relaxation behavior of porcine nasal septal cartilage at various isothermal temperatures.

energy. It can be inferred that some subtle structural change in cartilage occurs above 50°C and below 57°C , and this is consistent with storage modulus measurements (Fig. 5).

Shift Factor and Activation Energy for Relaxation on Porcine Septal Cartilage

Figure 7 is a plot of the shift factors (α_t) determined at various temperatures. The time based shift factor plot was curvilinear, consistent with the behavior predicted by the WLF equations [39]. Commercial software was used to determine calibration constants C_1 and C_2 . The shift factor

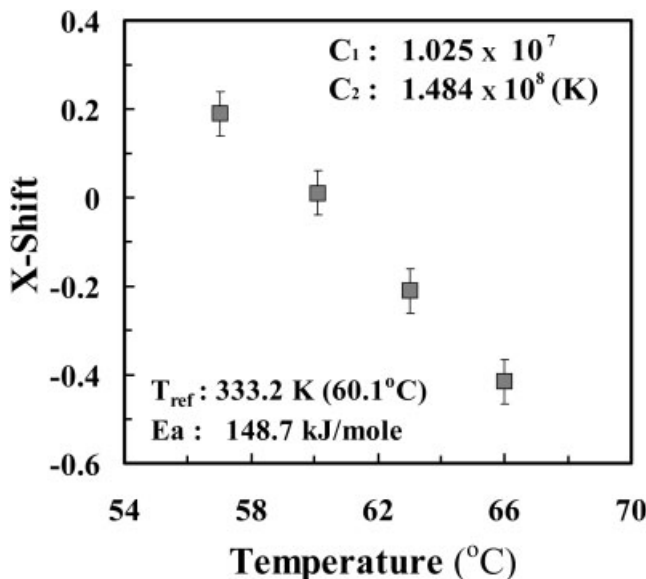


Fig. 7. Shift factor as a function of temperature relative to reference temperature 60.1°C .

was calculated based on a reference temperature, 60.1°C , that was estimated in previous differential scanning calorimetry studies [40] and this value is consistent with current stress relaxation measurement (Fig. 6). These calibration constants, ($C_1 = 1.025 \times 10^7$ and $C_2 = 1.484 \times 10^8$) were used to estimate the activation energy associated with the relaxation of porcine cartilage corresponding to the phase transition. The activation energy was calculated using an Arrhenius relation (Eq. 6) and the value obtained was estimated to be 148.7 kJ/mole .

DISCUSSION

While laser cartilage reshaping is performed using heating rates that are orders of magnitude faster than those used in this study, the characterization of cartilage thermoviscoelastic behavior at slow heating rates is still of direct relevance to studying shape change and phase behavior in this tissue. Optimization of the reshaping process requires an understanding of how stress and strain change in response to temperature, and differential scanning calorimetry and dynamic mechanical analysis are cornerstone techniques used in rheological science to study thermoviscoelasticity. This is the first study to systematically use DMTA and TTS to study stress relaxation in cartilage.

Multifrequency measurements of porcine nasal septal cartilage were obtained using a dynamic mechanical analyzer at several temperatures. Characteristic changes in mechanical properties suggestive of a phase transformation were identified between 50 and 67°C and these observations are consistent with previous studies, which used calorimetry to estimate the phase transition temperature range [40]. Anisotropic mechanical behavior of septal cartilage was observed, which is likely due to the inhomogeneous collagen fiber distribution and proteoglycan density. This degree of anisotropy was quantified by comparing the ratio of the storage moduli in transversely oriented specimen to longitudinally oriented one. This ratio allows us to estimate the viscoelastic behavior of cartilage in two directions based upon measurements in only one direction.

The mechanical changes observed using dynamic mechanical analysis were the result of a combination of effects that includes both water loss and changes in the intrinsic molecular structure of the material with heating. Identifying the relative contribution of each of these effects is challenging, particularly when the changes in material behavior are quite subtle. With increasing water loss, the storage moduli gradually decreased 12–17% after 5 minutes and 20–30% (after 10 minutes of evaporation at ambient conditions). In order to reduce the effect of water loss due to dehydration these measurements were recorded from each specimen within the first 5 minutes after it was placed in the furnace of the DMA (maintained at a constant user defined temperature). With this method, a significant change in the storage moduli was observed when specimens were evaluated at temperatures between 55 and 65°C . Accordingly, this transition temperature range was selected for use in TTS studies (and estimation of

activation energy), which are generally performed at temperatures near the phase transition.

Classic dynamic thermomechanical analysis (DMTA) measures stress and strain on a deformed specimen while the temperature increases as a function of time. Because of this relatively slow temperature ramp, biologic materials cannot be accurately studied because significant water evaporation occurs, which alone leads to profound changes in tissue properties independent of the effects of heat. To minimize the impact of dehydration on our measurements, instantaneous storage modulus was recorded at discrete temperatures over a very short time. This allowed estimation of transition temperatures accompanying even subtle changes in stress relaxation rate.

Basic mechanical properties also demonstrated frequency dependence in this transition temperature range; the transition temperature range increased slightly with higher oscillation frequencies. This is consistent with the earlier finding obtained from the study of relaxation behavior of cartilage [12,19,35]. At higher frequencies, the storage modulus decreases rapidly within a relatively narrow temperature range. Since this is the first study to the best of our knowledge that has examined frequency dependence of thermoviscoelasticity in cartilage, a broad range of oscillation frequencies were used. In general, there is a "roll-off" phenomenon for storage modulus with higher temperatures. This "roll-off" effect is steeper at higher frequencies and thus the transition temperature is more distinctly observed. Hence, performing these studies at higher frequencies allows more accurate determination of transition temperature. Overall, measurements of cartilage viscoelastic behavior provide fundamental data that can be incorporated into the WLF equation (in the frequency domain) and in turn allow the generation of master curves, which can be used to estimate the storage modulus at other frequencies.

Based on measurements of instantaneous storage moduli at series of discrete temperatures, the activation energy for stress relaxation was estimated using pure flexural deformations in specimens maintained in cantilever geometry. Assuming the validity of TTS, the WLF equation and Arrhenius relation can be used to estimate the activation energy (approximately 148 kJ/mole) associated with the mechanical relaxation of cartilage. Constants C_1 and C_2 for the WLF equation were estimated along with the empirical time base shift factor a_T . This estimated activation energy for stress relaxation is higher than the energy required for the evaporation of free water (41–44 kJ/mole) and the activation energy of water diffusion (30.6 kJ/mole) [14,18]. The value obtained in this study does support the hypothesis that stress relaxation in cartilage is a consequence of water diffusion as well as the adsorption and desorption of water by proteoglycans in cartilage matrix.

The activation energy for shape change/relaxation (phase transformation energy) was greater than that required to either evaporate water or adsorb/desorb water from PTGs [14,18]. In Sobol's studies [18], the activation energies of water diffusion and water evaporation were similar to one another: 27–41.4 kJ/g. The activation energy

for stress relaxation determined using DMTA is based upon measurements of macroscopic tissue properties that are influenced by experimental conditions such as thermal diffusion, water vaporization, and specimen geometry. The larger activation energy for stress relaxation relative to the evaporation energy can be interpreted in the context of tissue water content. For a low concentration of water, a large amount of energy is needed to facilitate water movement through the dense ECM and likewise liberate bound water from PTGs.

The mechanical properties of cartilage vary with time and temperature, and this behavior has been modeled using the empirically derived WLF equation. The storage modulus of cartilage decreased with decreasing the water content, and the elastic modulus is significantly reduced with dehydration. The mechanism of the cartilage reshaping is still uncertain and water whether bound to cartilage, free, or bound to minerals, plays an important role in thermally accelerated stress relaxation.

CONCLUSION

In this study, we determined the linear region of viscoelastic behavior of porcine cartilage and empirically analyzed the effect of temperature, water content, and orientation on mechanical behavior of cartilage. Using the WLF equation, the activation energy of this process was estimated based on the measure of the transition temperature region associated with relaxation. This value for the activation energy can be used to model viscoelastic behavior in cartilage and modified for different transition temperature regions (reference temperature). Further investigation of molecular mechanisms, which occur during laser irradiation, may provide insight into understanding how the reshaping process might be optimized.

ACKNOWLEDGMENTS

This paper was presented at the Annual Meeting of the American Society for Laser Medicine and Surgery in Atlanta, GA on April 11, 2002. Mr. Chae received the award for "The Best Student/Resident Paper (Poster Section)" and received a travel grant from the US Air Force Office of Scientific Research. Dr. Guillermo Aguilar acknowledges the support from the National Institutes of Health Research Grant HD-42057. The authors are grateful to Dr. Steven R Nutt at USC for the use of his instrumentation and Dr. Sergio H. Diaz and Mr. Hong Shen for their comments and technical assistance.

REFERENCES

1. Helidonis E, Sobol E, Kavvalos G, Bizakis J, Christodoulou P, Velegrakis G, Segas J, Bagratashvili V. Laser shaping of composite cartilage grafts. *Am J Otolaryngol* 1993;14(6):410–412.
2. Helidonis E, Volitakis M, Naumidi I, Velegrakis G, Bizakis J, Christodoulou P. The histology of laser thermo-chondroplasty. *Am J Otolaryngol* 1994;15:423–428.
3. Helidonis ES, Sobol EN, Velegrakis G, Bizakis J. Shaping of nasal septal cartilage with the carbon dioxide laser—a

- preliminary report of an experimental study. *Lasers Med Sci* 1994;9:51–54.
4. Jones N, Sviridov A, Sobol E, Omelchenko A, Lowe J. A prospective randomised study of laser reshaping of cartilage in vivo. *Lasers Med Sci* 2001;16(4):284–290.
 5. Omel'chenko AI, Bagratashvili VN, Sobol EN, Dmitriev AK. Mechanical examination of cartilage reshaped under laser radiation. *Adv Materials* 1999;3:56–63.
 6. Omel'chenko AI, Sobol EN, Sviridov AP, Harding SE, Jumel K, Walker R, Jones N. Opto-acoustic monitoring of laser corrections of the shape of porcine ear. *Russian J Quant Electron* 2000;11:823–826.
 7. Ovchinnikov Y, Sobol E, Svitushkin V, Shekhter A, Bagratashvili V, Sviridov A. Laser septochondrocorrection. *Arch Facial Plast Surg* 2002;4:180–185.
 8. Ovchinnikov YM, Nikiforova GN, Svitushkin VM, Gamov VP, Sobol EN, Bagratashvili VN, Omel'chenko AI, Sviridov AP, Naumidi I, Helidonis E. Changes in the cartilage shape under the action of laser irradiation. *Vestnik Otorinolaringologii* 1995;3:5–10.
 9. Sobol EN. Phase transformations and ablation in laser-treated solids. New York: John Wiley; 1995. 316–322.
 10. Wang Z, Pankratov MM, Perrault DF, Shapshay SM. Laser-assisted cartilage reshaping: In vitro and in vivo animal studies. *Proc SPIE* 1995;2395:296–302.
 11. Wong BJF, Milner TE, Kim HK, Nelson JS, Sobol EN. Stress relaxation of porcine septal cartilage during Nd:YAG ($\lambda = 1.32 \mu\text{m}$) laser irradiation: Mechanical, optical, and thermal responses. *J Biomed Opt* 1998;3(4):409–414.
 12. Wong BJF, Milner TE, Kim HK, Telenkov SA, Chew CF, Sobol EN, Nelson JS. Characterization of temperature-dependent biophysical properties during laser mediated cartilage reshaping. *IEEE J Sel Top Quantum Electron* 1999;5(4):1095–1102.
 13. Wong BJ, Milner TE, Harrington A, Ro J, Dao X, Sobol EN, Nelson JS. Feedback-controlled laser-mediated cartilage reshaping. *Arch Facial Plast Surg* 1999;1(4):282–287.
 14. Bagratashvili VN, Sobol EN, Sviridov AP, Popov VK, Omel'chenko AI, Howdle SM. Thermal and diffusion processes in laser-induced stress relaxation and reshaping of cartilage. *J Biomech* 1997;30(8):813–817.
 15. Basu R, Wong BJ, Madsen SJ. Wavelength-dependent scattering of light during Nd:YAG laser heating of porcine septal cartilage. *Proc SPIE* 2001;4257:221–230.
 16. Sobol EN, Kitai MS, Jones N, Sviridov AP, Milner T, Wong BJF. Heating and structural alterations in cartilage under laser radiation. *IEEE J Quant Electron* 1999;35(4):532–539.
 17. Sobol E, Omel'chenko A, Mertig M, Pompe W. Scanning force microscopy of the fine structure of cartilage irradiated with a CO₂ laser. *Lasers Med Sci* 2000;15:15–23.
 18. Sobol E, Sviridov A, Omel'chenko A, Bagratashvili V, Kitai M, Harding SE, Jones N, Jumel K, Mertig M, Pompe W, Ovchinnikov Y, Shekhter A, Svitushkin V. Laser reshaping of cartilage. *Biotechnol Genet Eng Rev* 2000;17:553–578.
 19. Sviridov A, Sobol EN, Jones NS, Lowe J. Effect of holmium laser radiation on stress, temperature, and structure alterations in cartilage. *Lasers Med Sci* 1998;13:73–77.
 20. Wong BJF, Milner TE, Anvari B, Sviridov A, Omel'chenko A, Bagratashvili VV, Sobol EN, Nelson JS. Measurement of radiometric surface temperature and integrated back-scattered light intensity during feedback controlled laser-assisted cartilage reshaping. *Lasers Med Sci* 1998;13:66–72.
 21. Wong BJ, Milner TE, Kim HK, Chao K, Sun CH, Sobol EN, Nelson JS. Proteoglycan synthesis in porcine nasal cartilage grafts following Nd:YAG ($\lambda = 1.32 \mu\text{m}$) laser-mediated reshaping. *Photochem Photobiol* 2000;71(2):218–224.
 22. Youn J-I, Vargas G, Ducros MG, Telenkov SA, Wong BJ, Milner TE. Thermally induced birefringence changes in cartilage using polarization-sensitive optical coherence tomography. *Proc SPIE* 2001;4257:213–220.
 23. Chao KKH, Wong BJF. Thermomechanical analysis of lagomorph nasal septal cartilage during Nd:YAG laser irradiation. 2001; submitted for publication.
 24. Gaon MD, Wong BJF. Measurement of the elastic modulus of porcine septal cartilage specimens following Nd:YAG laser treatment. *Proc SPIE* 2000;3907:370–379.
 25. Karamzadeh AM, Rasouli A, Tanenbaum BS, Milner TE, Nelson JS, Wong BJ. Laser-mediated cartilage reshaping with feedback-controlled cryogen spray cooling: Biophysical properties and viability. *Lasers Surg Med* 2001;28(1):1–10.
 26. Omel'chenko AI, Bagratashvili NV, Dmitriev AK, Sobol EN. Acoustic control of laser shaping of cartilage. *Laser spectroscopy and optical diagnostics: Novel trends and applications in laser chemistry, biophysics, and biomedicine* 1999;3732:312–319.
 27. Sobol EN, Sviridov A, Bagratashvili VV, Omel'chenko A, Ovchinnikov Y, Shekhter A, Downes S, Howdle S, Jones N, Lowe J. Stress relaxation and cartilage shaping under laser radiation. *Proc SPIE* 1996;2681:358–363.
 28. Youn JI, Telenkov SA, Kim E, Bhavaraju NC, Wong BJ, Valvano JW, Milner TE. Optical and thermal properties of nasal septal cartilage. *Lasers Surg Med* 2000;27(2):119–128.
 29. Wong BJ, de Boer JF, Park BH, Chen Z, Nelson JS. Optical coherence tomography of the rat cochlea: Preliminary investigations. *Proc SPIE* 1999;3590:261–264.
 30. Wong BJ, Milner TE, Anvari B, Sviridov AP, Omel'chenko AI, Vagratashvili V, Sobol EN, Nelson JS. Thermo-optical response of cartilage during feedback-controlled laser-assisted reshaping. *Proc SPIE* 1997;2970:380–391.
 31. Bagratashvili VN, Bagratashvili NV, Gapontsev VP, Makhmutova GS, Minaev VP, Omel'chenko AI, Samartsev IE, Sviridov AP, Sobol EN, Tsykina SI. Change in the optical properties of hyaline cartilage heated by the near-IR laser radiation. *Kvantovaya Elektronika Moskva* 2001;31(6):534–538.
 32. Madsen SJ, Chu E, Wong BJF. The optical properties of porcine nasal cartilage. *IEEE J Sel Top Quantum Electron* 1999;5:1112–1133.
 33. Dark ML, Perelman LT, Itzkan I, Schaffer JL, Field MS. Physical properties of hydrated tissue determined by surface interferometry of laser-induced thermoelastic deformation. *Phys Med Biol* 2000;45(2):529–539.
 34. Bagratashvili V, Bagratashvili N, Sviridov A, Sobol E, Omel'chenko A, Tsykina S, Gapontsev V, Samartsev I, Feldchtein F, Kuranov R. Kinetics of water transfer and stress relaxation in cartilage heated with 1.56 μm fiber laser. *Proc SPIE* 2000;3914:102–107.
 35. Diaz-Valdes S, Lavernia EJ, Wong BJ. Mechanical behavior of cartilage during laser irradiation. *Proc SPIE* 2001;4257:192–197.
 36. Chao KK, Burden MA, Wong BJ. Dynamic changes in the elastic modulus of lagomorph nasal septal cartilage during Nd:YAG ($\lambda = 1.32 \mu\text{m}$) laser irradiation. *Proc SPIE* 2001;4257(2001):247–254.
 37. Chae Y, Diaz-Valdes S, Lavernia EJ, Wong BJ. Finite element analysis of thermal residual stress and temperature changes in cartilage during laser radiation. *Proc SPIE* 2001;4257:255–268.
 38. Wong BJF, Chao K, Kim HK, Chu EA, Dao X, Gaon M, Sun C-H, Nelson JS. The porcine and lagomorph septal cartilages: Models for tissue engineering and morphologic cartilage research. *Am J Rhino* 2001;15:109–116.
 39. Ferry JD. *Viscoelastic properties of polymers*. Third edition. New York: John Wiley & Sons; 1980.
 40. Chae Y, Lavernia EJ, Wong BJ. Effect of water content on specific heat capacity of porcine septum cartilage using temperature modulated DSC (differential scanning calorimetry). *Proc SPIE* 2002;4617:57–66.